Presented at the 25th European PV Solar Energy Conference and Exhibition, 6-10 September 2010, Valencia, Spain

SIMPLIFYING THE MANUFACTURING OF N-TYPE SILICON SOLAR CELLS WITH SCREEN-PRINTED ALUMINIUM-ALLOYED REAR EMITTER

Michael Rauer[1], Christian Schmiga[1], Karsten Meyer[2], Jan Lossen[2], Hans-Joachim Krokoszinski[2], Martin Hermle[1] and Stefan W. Glunz[1]

[1]Fraunhofer Institute for Solar Energy Systems (ISE)
Heidenhofstraße 2, 79110 Freiburg, Germany
Phone: +49(0)761/4588-5921, Fax: +49(0)761/4588-9250,
E-mail: michael.rauer@ise.fraunhofer.de

[2]Bosch Solar Energy AG
Wilhelm-Wolff-Straße 23, 99099 Erfurt, Germany

ABSTRACT: This work focuses on simplifying the fabrication process of our near-industrial *n*-type silicon solar cells with screen-printed aluminium-alloyed rear emitter. We investigate the structural and electrical properties of Al emitters alloyed on differently prepared Si surfaces. We demonstrate that the formation of a proper emitter neither requires a planar nor a non-diffused rear surface, thus allowing both-sided surface texturing and both-sided phosphorous doping during the n^+ front surface field diffusion without the need of an additional protecting rear masking layer. On textured surfaces a careful choice of the printing and alloying conditions is essential to obtain Al-p^+ emitters without shunts in form of locally non-alloyed regions. By adjusting the alloying conditions or by applying a simple rear surface conditioning step, shunts can be effectively prevented, thereby simultaneously increasing the internal reflectance and reducing the Al-p^+ emitter saturation current density. Al alloying on P-diffused rear surfaces is shown to be uncritical. In summary, we demonstrate that Al alloying for p^+ emitter formation can be easily realised on textured and P-diffused surfaces leading to a much more flexible fabrication of our *n*-type silicon solar cells.
Keywords: Industrial Cell Processing, Aluminium-alloyed Emitter, *n*-type Silicon Solar Cells

1 INTRODUCTION

The fabrication of high-efficiency silicon solar cells sets high demands on the quality of the bulk material. Using *p*-type boron-doped Czochralski-grown silicon does not satisfy these demands due to the detrimental effect of boron-oxygen-related light-induced degradation [1]. The further purification of the silicon by methods like zone melting is expensive and industrially unprofitable. Therefore an alternative approach is pursued in industrial cell production, which is based on *n*-type phosphorous-doped Si, thereby taking advantage of the superior electrical properties due to higher and more stable diffusion lengths [2]. However, to benefit from the excellent material properties, an industrially applicable emitter fabrication method is necessary, directing the intention to alloying of screen-printed aluminium pastes [3]. For large-area solar cells featuring a full-area screen-printed Al-alloyed rear emitter, we have recently reported efficiencies of 18.2 % [4] (Figure 1, total area 148.5 cm^2), which we have further increased to a remarkably high value of 19.3 % [5]. For small-area solar cells we have achieved efficiencies exceeding 20 %, demonstrating the high potential of this n^+np^+ cell structure [6].

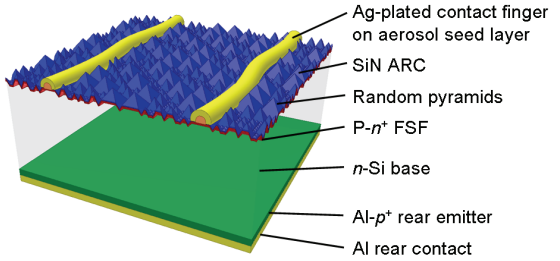

Figure 1: Structure of our near-industrial n^+np^+ *n*-type Si solar cell with screen-printed aluminium-alloyed rear p^+ emitter [4].

In this work, we focus on simplifying the fabrication process of our large-area *n*-type solar cells with Al-p^+ rear emitter. For process simplification a closer look on the solar cell processing sequence, which is described in [4], is obligatory.

In detail: After saw damage etching, an oxide mask is prepared on the rear side to provide protection for the subsequent texturing with random pyramids and the phosphorous front surface field (FSF) diffusion. Then the oxide layer is removed in a HF solution. Subsequently, an antireflection silicon nitride layer is deposited on the front by plasma enhanced chemical vapour deposition (PECVD) and the seed layer for the front side metallisation is printed using the aerosol technique. After full-area screen-printing of aluminium paste onto the rear, a co-firing step is carried out to form the front contacts and to simultaneously alloy the Al-p^+ rear emitter. Finally, the seed layer is thickened by means of light-induced silver plating. The resulting cell structure is shown in Figure 1.

As the processing sequence is already quite straightforward, the possibilities for simplifying the solar cell manufacturing are very limited. Our approach therefore is based on omitting rear side oxide masking, which has primarily been included to enable single-sided texturing and a single-sided phosphorous diffusion of the n^+ front surface field (FSF). Our investigations therefore concern two main issues: (i) the alloying of screen-printed Al pastes on textured surfaces and (ii) the overcompensation of the rear P diffusion by Al alloying. Though this simplification procedure is already used in the fabrication of conventional *p*-type solar cells with Al back surface field (BSF) [7, 8], the alloying conditions cannot be transferred to *n*-type solar cells for the p^+ emitter formation without restrictions [9].

2 ALUMINIUM ALLOYING ON TEXTURED SURFACES

2.1 Sample Fabrication

In the course of this study, we fabricated simple test samples to investigate Al alloying on textured surfaces using the processing sequence shown in Figure 2. As starting material we used saw damage-etched Si wafers. After texturing with random pyramids, the samples were split into three groups to prepare different surface conditions. Whereas the first fraction was retained (*surface condition a*), the second fraction was exposed to KOH solution for 90 s to round off the vertices and edges of the pyramids (*surface condition b*). The third fraction was mechanically grinded to remove the pyramids, thereby inducing a faint grinding damage (*surface condition c*). Figure 3 shows scanning electron microscope (SEM) images of the sample surfaces after these preparation steps. In addition to textured samples, we took along shiny-etched Si wafers as references (*surface condition d*).

After surface preparation a commercially available aluminium paste was screen-printed onto the entire rear surface, thereby using an amount of 7 mg/cm² and 16 mg/cm² (measured after drying). For the formation of the Al-p^+ region, the samples were subsequently fired in a conveyor belt furnace at a peak temperature of 900°C. Two different peak temperature times were applied here, which were adapted to the respective Al amount [10-12]: A short one (4 s) for the lower and a more extended one (7 s) for the higher Al amount. To simplify matters, these printing and firing conditions are referred to as *alloying conditions A* and *B*, see Figure 2.

To enable a distinct characterisation of the emitter homogeneity, paste residuals and the Al-Si eutectic layer were subsequently etched off in hydrochloric acid.

2.2 Homogeneity of Al-p^+ Emitter

The formation of a non-shunted and homogeneous Al-p^+ region is a crucial point for the fabrication of *n*-type Si solar cells with Al rear emitter. Therefore, the transfer of Al alloying from planar to textured surfaces has to be done carefully. Figure 4 shows SEM pictures of a surface formerly textured with random pyramids (surface condition a) after Al alloying using alloying conditions A. It is clearly visible that part of the surface still exhibits sharp-edged pyramids. Due to the steep ascent of the Al-p^+ doping profile against the Si bulk, a well-defined contrast in cross-sectional SEM images indicates the Al-p^+ / Si interface and can therefore be used for homogeneity investigations. Applying alloying conditions A, the Al-p^+ region does not form homogeneously along the surface which can lead to shunts within the pointed valleys between two pyramids. This may be attributed to the size of the Al paste particles which is too large to provide full coverage of the valleys by screen-printing. Therefore dissolving of Si into the Al-Si melt and epitaxial Si recrystallisation during alloying does not range deep enough to affect the pyramid valleys as well.

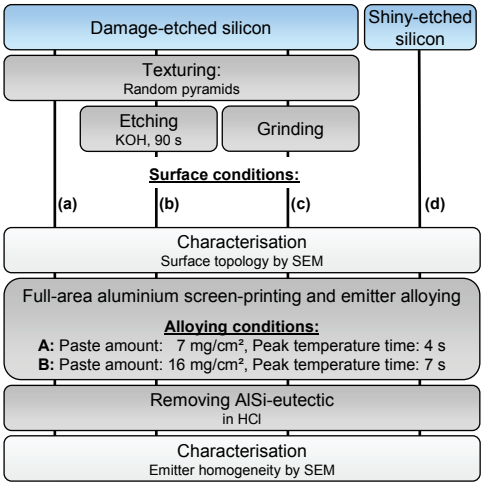

Figure 2: Processing sequence of the surface preparation before aluminium screen-printing.

Our approach for an improved emitter formation is based on adapting the printing and firing conditions in order to increase the amount of dissolved and recrystallised Si [12]. Using alloying conditions B leads to a smooth surface, as the former pyramidal texture is totally flattened during the alloying process, see Figure 5. As a result the Al-p^+ region forms very homogeneously without any shunts.

For industrial cell fabrication Al alloying often has to be adjusted to other processes, *e.g.* the firing of the front side metallisation, prohibiting a free choice of the alloying conditions. Therefore other approaches for Al alloying on textured surfaces, based on curing the surface after texturing, were performed: (i) broadening the critically pointed valleys between the pyramids by a short chemical etching step in KOH solution (surface condition b) and (ii) flattening the pyramids by mechanical grinding (surface condition c), see Figure 3b and 3c, respectively. After alloying using conditions A the surface hence possesses an uneven, wavy topology, see Figure 6. However, the sharp edged pyramids vanish and the Al-p^+ region

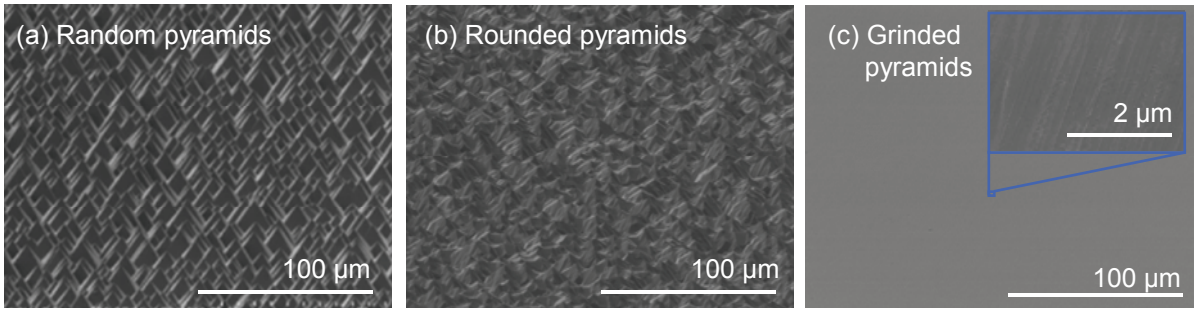

Figure 3: SEM top view images of the sample surfaces after preparation. Labels (a) to (c) are assigned according to Figure 2. The inset in image (c) shows a close-up image of the grinding damage.

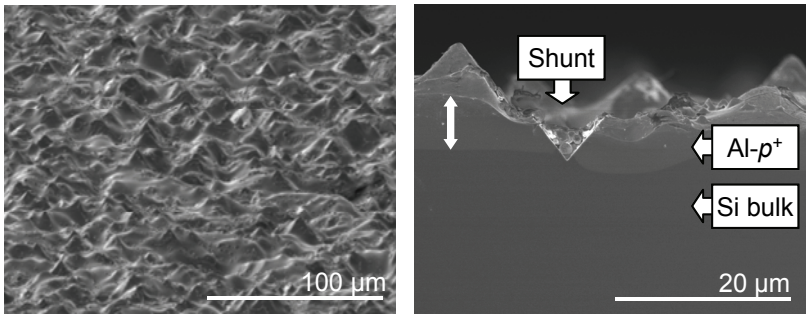

Figure 4: SEM top view (*left*) and cross-sectional image (*right*) of a surface formerly textured with random pyramids (surface condition a) after alloying using conditions A and paste removal. Part of the surface still features sharp-edged pyramids (left). The Al-p^+ region does not form continuously due to insufficient alloying within the pointed valleys between the pyramids (right).

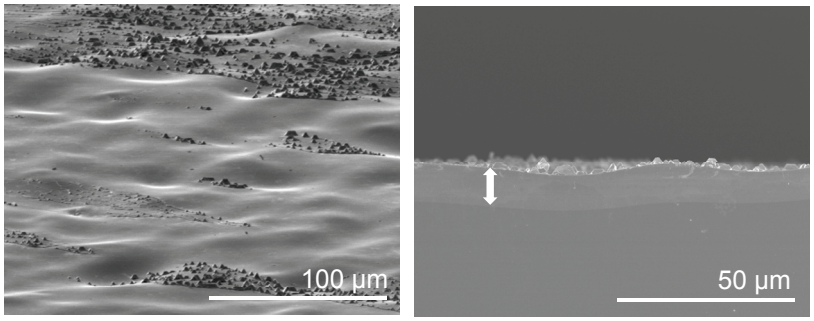

Figure 5: SEM top view (*left*) and cross-sectional image (*right*) of a surface formerly textured with random pyramids (surface condition a) after alloying using conditions B and paste removal. The adaption of the printing and firing conditions leads to the complete dissolving of the pyramids and a homogeneous Al-p^+ formation.

forms continuously. Comparing the topology and emitter homogeneity of these samples to the shiny-etched reference sample (surface condition d, Figure 6 d) indicates that the rough surface is not caused by the surface preparation itself but by the alloying conditions. This implies that for shunt prevention not the entire pyramidal texture but only the critical spots have to be removed.

Although involving additional process steps, chemical etching or mechanical grinding represent explicit process simplifications. Instead of demanding the fabrication of etch masks by means of thermal oxidation, PECVD layers or inkjet techniques and a subsequent lift-off etching, these approaches only require the deposition of a protective SiN_x layer on the front side, which is already implemented in the solar cell processing sequence as the front side antireflection coating. Therefore no significant changes in the solar cell fabrication process are necessary.

2.3 Internal Reflectance

Aluminium layers exhibit strong parasitic absorption due to plasmon stimulation which reduces the internal reflectance R_i, *i.e.* the reflectance in the long wavelength range at the solar cell's rear, of our *n*-type Si solar cells with Al-alloyed rear p^+ emitter [6, 13].

To evaluate the influence of the alloying conditions on the internal reflectance, a 2 µm thick Al metal layer was evaporated on top of the Al-doped p^+ regions. Hence the evaporated Al layer replaces the screen-printed back side metallisation for the reflectance measurements. This substitution is suitable since the surface morphology of the Al-doped p^+ region, including pyramidal Al-containing crystalline structures [10, 11, 14], is completely preserved. Moreover, after screen-printing and alloying, the surface of the Al-doped p^+ region is covered by a compact layer with eutectic composition [12]. This eutectic layer is composed heterogeneously, *i.e.* Si and Al segregate into two separate phases when the Al-Si melt solidifies at the eutectic point. As the eutectic layer consists of Al to a large percentage, the Al-doped p^+ region is predominantly covered by an Al metal layer which approximately is similar to the evaporated Al layer. We could verify the substitution of the back side metallisation via reference measurements.

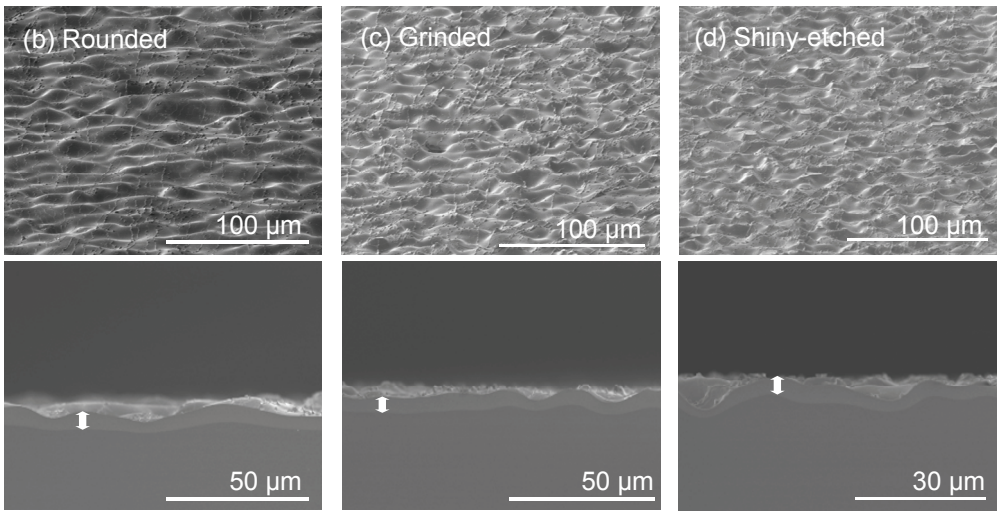

Figure 6: SEM top view (*top*) and cross-sectional image (*bottom*) of samples after different surface preparations and Al alloying using conditions A and paste removal. Labels refer to surface conditions.

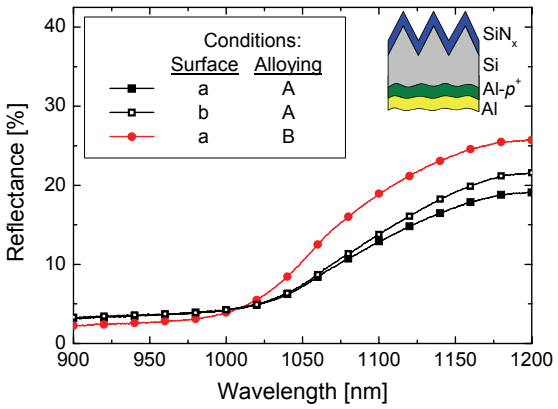

Figure 7: Reflectance in the long wavelength range after alloying using alloying conditions A and B, respectively, and Al metal evaporation. Full symbols refer to rear surfaces that were formerly textured (surface condition a), hollow symbols to additionally KOH etched rear surfaces (surface condition b).

The reflectance in the long wavelength range is shown in Figure 7 for samples that formerly featured a textured or a textured and KOH-etched rear surface (surface condition a and b, respectively) after alloying using conditions A or B. It can be seen that the roughness of the Al-p^+ region caused by alloying conditions A on textured surfaces strongly reduces the internal reflectance R_i. This may be attributed to enhanced parasitic absorption in the rear Al metal which is known to increase with surface roughness [15]. The implementation of a short etching or grinding step leads to a slightly improved internal reflectance due to the smoother Al-p^+ surface after alloying A. The more accurate smoothing of the Al-p^+ surface by the adaption of the alloying conditions (alloying condition B), however, results in a significantly larger increase in R_i. Therefore in addition to shunt prevention, the application of adapted alloying or simple after-treatment steps also could lead to an increase in the short-circuit current density of the solar cell.

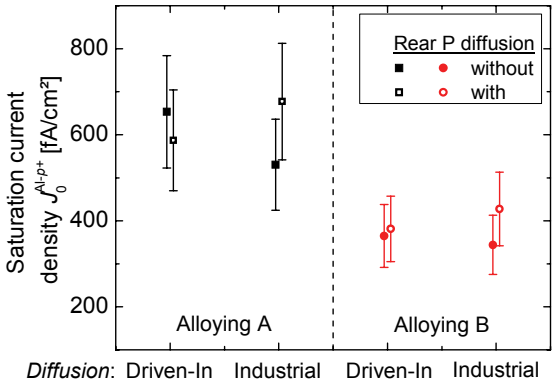

Figure 8: Saturation current density $J_0^{Al\text{-}p+}$ as a function of Al alloying conditions and P diffusion. Full symbols refer to samples without additional rear P diffusion and hollow symbols to samples with diffusion, respectively.

3 OVERCOMPENSATION OF REAR PHOSPHOROUS DIFFUSION

Besides demanding Al alloying on textured surfaces, omitting the rear side oxide masking leads to a both-sided $POCl_3$ diffusion during the formation of the n^+ FSF. Thus the second part of this work deals with overcompensating the rear P diffusion.

3.1 Sample Fabrication

We fabricated simple lifetime test samples [10] to investigate the overcompensation of the rear P diffusion. We used shiny-etched float-zone (FZ) Si with a resistivity of 100 Ωcm. As the emitter properties do not depend on the kind of bulk doping, we chose *p*-type Si for evaluation reasons. To directly characterise the influence of the rear P diffusion, the samples were split into two groups, one group receiving a single-sided rear diffusion owing to an additional front thermal oxide mask, the other group remaining undiffused. Two different P-n^+ diffusion profiles were applied here: An *industrial-type doping profile* with a sheet resistance of 65 Ω/sq and a surface doping concentration of $1{\cdot}10^{20}$ cm^{-3}, and a *driven-in doping profile* with similar sheet resistance and a surface doping concentration of $5{\cdot}10^{19}$ cm^{-3}. Subsequently the oxide mask is etched off and a PECVD SiN_x layer (refractive index 2.1) is deposited to passivate the front side. For the alloying of the screen-printed Al paste conditions A and B were applied, see section 2.1. Finally, the samples were treated to an etching step in hydrochloric acid to remove paste residuals and the Al-Si eutectic layer.

3.2 Results and Discussion

Quasi-steady-state photoconductance (QSSPC) measurements were performed to determine the Al-p^+ emitter saturation current density $J_0^{Al\text{-}p+}$ [10] for samples with and without preceded rear P diffusion, see Figure 8. It is clearly visible that the additional rear diffusion does not affect the electrical properties, as $J_0^{Al\text{-}p+}$ differences are within measurement uncertainties. In particular, there is no difference observable for the shallow and the driven-in P doping profiles. This can be attributed to the segre-

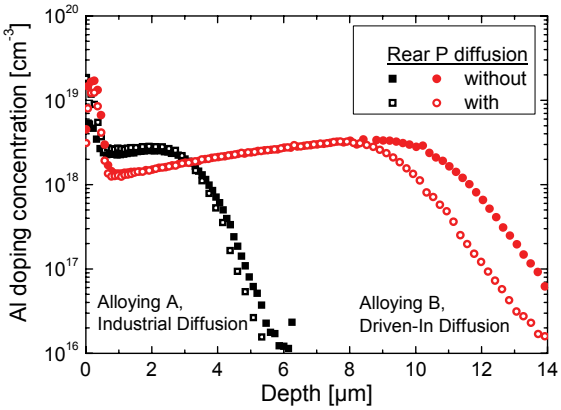

Figure 9: ECV doping profiles of Al-p^+ regions with (hollow symbols) and without (full symbols) additional rear side P diffusion. Differences in the doping profiles result from small variations of the printed Al amount.

gation of the P atoms into the rear Al-Si eutectic during alloying [7], the latter being afterwards removed by HCl etching. As a consequence, no P-related dip can be detected in the electrochemical capacitance voltage (ECV) measurements of the Al-p^+ doping profiles which are in good agreement, see Figure 9. In summary, the implementation of a both-sided P diffusion does not result in electrical losses and thus can be considered to be uncritical.

The comparison of the $J_0^{\text{Al-}p+}$ values for alloying conditions A and B shows that the adaption of the printing and firing conditions can lead to an enhancement of the open-circuit voltage. This is consistent with the increase in the thickness of the Al-p^+ regions, enhancing the electron screening from the recombination active surface [10, 11].

Therefore the application of adapted alloying conditions not only leads to an improved internal reflectance and avoids shunts, but can also raise the open-circuit voltage of our *n*-type Si solar cells.

4 APPLICATION TO SOLAR CELLS

In order to evaluate the simplified fabrication on solar cell level, we fabricated large-area *n*-type Czochralski-grown Si solar cells with Al-alloyed rear emitter [5], thereby applying both-sided texturing and both-sided phosphorous doping during the FSF diffusion. As the front side metallisation and the Al-p^+ emitter were co-fired, the alloying conditions were preset, resembling alloying conditions A, see section 2.1. Therefore, preceding to Al screen-printing the rear texture was conditioned in KOH solution to round the pyramidal structures and avoid non-alloyed regions, see section 2.2.

Benefiting from an improved front surface scheme, we could achieve a notably high solar cell efficiency of 18.5 %. Thereby the fill factor value of 79.6 % proves the high junction quality, demonstrating the successful implementation of the processing simplification into the fabrication of our *n*-type solar cells.

5 SUMMARY

We have investigated the alloying of screen-printed Al pastes on textured and phosphorous-diffused surfaces for a simplified and more flexible fabrication of our *n*-type Si solar cells with Al-p^+ rear emitter.

We demonstrate that on randomly textured surfaces the alloying conditions have to be chosen carefully to avoid emitter shunts in form of locally non-alloyed regions. However, by adjusting the alloying conditions we achieve a much smoother surface featuring a non-shunted and homogeneous Al-p^+ emitter, as the surface texture has completely been dissolved. For co-firing processes with preset alloying conditions we propose simple after-treatment steps to effectively prevent shunts without causing significant processing changes.

The application of adapted alloying conditions or simple after-treatment leads to an improved internal reflectance, promising a gain in the short-circuit current density. In addition, the increased Al-p^+ thickness, that is associated with adapted alloying, can lead to a gain in the open-circuit voltage by decreasing the Al-p^+ emitter saturation current density.

Furthermore, we show that overcompensation of P-doped surfaces by Al alloying is uncritical and does not result in electrical losses. In summary, we demonstrate that Al alloying can be easily realised on textured and P-diffused surfaces.

The results of this study can be used for a simplified and much more flexible fabrication of our large-area *n*-type solar cells with Al-alloyed rear emitter. This was demonstrated by achieving solar cell efficiencies of 18.5 %, proving the successful implementation of the processing simplification on solar cell level. In addition to *n*-type Si solar cells, the results of this study are interesting for applications to *p*-type Si solar cells with Al back surface field.

ACKNOWLEDGEMENTS

The authors would like to thank A. Leimenstoll and F. Schätzle for cleanroom processing. A. Filipovic is gratefully acknowledged for screen-printing and J. Zielonka for SEM measurements.

REFERENCES

[1] S.W. Glunz, S. Rein, J.Y. Lee, W. Warta, J. Appl. Phys. 90 (1), 2001; 2397

[2] A. Cuevas, M.J. Kerr, C. Samundsett , Vol. 81, No.26, 2002; 4952

[3] C. Schmiga, H. Nagel, J. Schmidt, Progress in Phototovoltaics, **14**, 2006; 533

[4] C. Schmiga, M. Hörteis, M. Rauer, K. Meyer, J. Lossen, H.-J. Krokoszinski, M. Hermle, S.W. Glunz, Proc. 24th EPVSEC, Hamburg, Germany, 2009; 1167

[5] C. Schmiga, M. Rauer, M. Rüdiger, K. Meyer, J. Lossen, H.-J. Krokoszinski, M. Hermle, S.W. Glunz, *Aluminium-doped p^+ Silicon for Rear Emitters and Back Surface Fields: Results and Potentials of Industrial n- and p-type Solar Cells*, this conference

[6] C. Schmiga, M. Hermle, S.W. Glunz, Proc. 23rd EPVSEC, Valencia, Spain, 2008; 982

[7] A. Schneider, R. Kopecek, G. Hahn, S. Noel, P. Fath, Proc. 31st IEEE PVSC, Florida, USA, 2005; 105

[8] D. Biro, S. Mack., A. Wolf, A. Lemke, U. Belledin, D. Erath, B. Holzinger, E.-A. Wodke, M. Hofmann, L. Gautero, S. Nold, J. Rentsch, R. Preu, Proc. 34rd IEEE PVSC, Philadelphia, USA, 2009

[9] H. Nagel, C. Schmiga, B. Lenkeit, G. Wahl, W. Schmidt, Proc. 21st EPVSEC, Dresden, Germany, 2006; 1228

[10] M. Rauer, C. Schmiga, M. Hermle, S.W. Glunz., Proc. 25th EPVSEC, Hamburg, Germany, 2009; 1059

[11] M. Rauer, C. Schmiga, M. Hermle, S.W. Glunz, Phys. Status Solidi A, 2009, Volume 207, Issue 5, 2010; 1249

[12] F. Huster, Proc. 20th EPVSEC, Barcelona, Spain, 2005; 1466

[13] D. Kray, M. Hermle, S.W. Glunz, Prog. Photovolt: Res. Appl. 2008; **16**: 1-15

[14] R. Bock, J. Schmidt, R. Brendel, H. Schuhmann, M. Seibt, J. Appl. Phys. **104**, 2008; 043701

[15] A.A. Maradunin, D.L. Mills, Phys. Rev. B, Vol. 11, 1975; 1392